科技部補助專題研究計畫成果報告
期末報告

水溶性碳六十衍生物與聚醯胺乙二胺樹枝狀分子在基因轉染上的研究(第 2 年)

計 畫 類 別 ：個別型計畫
計 畫 編 號 ：NSC 100-2113-M-040-007-MY2
執 行 期 間 ：101 年 08 月 01 日至 102 年 12 月 31 日
執 行 單 位 ：中山醫學大學應用化學系（所）

計 畫 主 持 人：朱智謙

計畫參與人員：碩士級-專任助理人員：洪澄祥
碩士班研究生-兼任助理人員：賴鈺森
碩士班研究生-兼任助理人員：江倢瑩

處 理 方 式 ：
1.公開資訊：本計畫涉及專利或其他智慧財產權，2 年後可公開查詢
2.「本研究」是否已有嚴重損及公共利益之發現：否
3.「本報告」是否建議提供政府單位施政參考：否

中 華 民 國 103 年 03 月 21 日

中 文 摘 要 ： 本研究中，我們成功的以點擊化學反應製備出一系列以碳六十為核心的兩性樹枝狀聚醯胺乙二胺分子。此兩性碳六十衍生物可以在水中自組裝形成核殼狀的奈米粒子，並且可以作為 DNA 載體，在極低的氮磷比下，將 DNA 運送至兩種細胞中，其細胞吞噬效率與市售的高分子載體 Turbofect 相當接近，而從綠色螢光蛋白質的表現，我們證實其基因轉染能力。透過分子結構的調整，提高結構降解與 DNA 釋放效率，將可提升整體基因轉染效力。

中文關鍵詞： 兩性樹枝狀分子、富勒烯、基因傳遞、聚醯胺乙二胺、自組裝、點擊化學

英 文 摘 要 ： In this research, we successfully performed a ’click’ synthesis of amphiphilic poly(amido amine) (PAMAM) dendron-bearing fullerenyl conjugate (C60G1) using a copper(I)-catalyzed azide-alkyne cycloaddition (CuAAC) reaction. The strong hydrophobicity of the C60 moiety induces self-assembly of C60G1 into core-shell-like ’pseudodendrimers’ with a uniform size distribution and positively charged peripherals. The pseudodendrimers were well-characterized by atomic force microscopy (AFM), transmission electron microscopy (TEM), and dynamic light scattering (DLS). On the basis of electrostatic interactions, the polycationic C60G1 assembly can serve as a non-viral gene vector. An ethidium bromide displacement assay and agarose gel electrophoresis both indicated that C60G1 assembly forms stable complexes with the cyclic reporter gene (pEGFP-C1) at low nitrogen-to-phosphorous (N/P) ratios. AFM analysis revealed a dynamic complex formation process, and confirmed the synthesis of C60G1/pEGFP-C1 hybrids with a particle dimensions less than 200 nm. Fluorescence microscopy and flow cytometry revealed that 51% of HeLa and 43% of MCF 7 cells are positive to the YOYO-1-labeled hybrids at an N/P ratio of 2, and in vitro gene transfection revealed an approximately 50% EGFP expression at N/P = 32, relative to TurboFect-mediated delivery.

英文關鍵詞： Amphiphilic Dendrons, Fullerene, Gene Delivery, PAMAM, Self-Assembly, Click Chemistry

Introduction and research motivation

Poly(amido amine) (PAMAM) dendrimers are considered to be biocompatible, non-immunogenic drug and gene vehicles because they demonstrate remarkable effectiveness for in vitro and in vivo medication delivery.[1-4] However, PAMAM toxicity profiles are problematic for biomedical applications because of the presence of polycationic substituents, and their persistence in cells. Alternatively, using the dendron architectures in which a hydrophobic group at the focal point encourages self-assembly of the resulting amphiphilic dendrons into large "pseudodendrimers".[5-7] This supramolecular strategy is a novel concept in the field of dendrimer-mediated nucleic acid delivery.[8,9] In addition, this type of dendrimers combing the characteristics of cationic polymers and lipids, can give rise to synergistic effects in gene delivery.[10,11]

Carbon-based nanomaterials, such as fullerenes, nanotubes, and graphene have attracted considerable interest for their biomedical applications, because of their unique in vitro and in vivo biodistributions and functionalities.[12-15] In particular, fullerene derivatives that combine 3-dimensionality with defined physiochemical properties are promising candidates for the preparation of bioactive molecules with unique biodistributions.[16] Nakamura and coworkers pioneered stable DNA-C_{60} hybrids that are capable of effective cell transfection, not only of mammalian cells, but also of pregnant female ICR mice, with distinct organ selectivity; they conducted a systematic structure-activity relationship (SAR) investigation on a library of 22 cationic fullerene derivatives, and proposed that an appropriate hydrophilic-lipophilic balance (HLB) is essential to synthesize DNA-fullerene complexes for effective gene transfection.[17-20]

Although variations in transfection protocol and cell type can dramatically affect transfection efficiency, the size and morphology of the DNA-vector complexes are also critical parameters to accomplish efficient gene delivery. Pristine C_{60} is an extremely solvophobic and water-insoluble molecule, and thus the presence of hydrophilic pendant groups confer greater solubility in aqueous media, essential for biological applications.[21-23] However, the amphiphilic nature of such water-soluble C_{60} derivatives usually results in spontaneous self-aggregation in aqueous media. Thus, careful manipulation of the amphiphilic counterpart is necessary to achieve a more favorable HLB to form stable gene vehicles with appropriate shape and morphology (e.g., spheroid or vesicle-like), thus facilitating DNA complexation, cellular uptake, and gene transfection.[24-27]

In the current study, we demonstrate a facile synthesis of amphiphilic PAMAM dendron-bearing fullerene derivative, by using an efficient Cu(I)-catalyzed azide-alkyne cycloaddition (CuAAC).[28] We found that the click cluster, interconnecting the diazido-functionalized fullerene and PAMAM dendrons bearing a propargyl focal point via a 1,4-triazole linkage, is highly water-soluble and is readily prepared in high yield without the need for chromatographic purification. Amphiphilic dendrons containing an extremely hydrophobic fullerene moiety and a hydrophilic PAMAM dendritic scaffold, favor the formation of nanoparticles with a uniform size distribution in water. AFM analysis revealed that these particles could condense plasmid DNA into stable complexes with desirable dimensions, at low nitrogen-to-phosphorus (N/P) ratios. Moreover, the fullerodendron assembly also exhibited remarkable gene delivery efficiency towards the target cell lines.

Experimental methods

Materials and instruments

Pure C_{60} was purchased from Uni-onward Corporation and used as received. Other chemicals used for

organic synthesis were obtained as high-purity reagent-grade chemicals from either Acros or Sigma-Aldrich and used without further purification. Organic solvents were AR grade and purchased from either Mallinckrodt or Echo chemicals. Ethylenediamine (EDA) and dichloromethane (DCM) were dried over calcium hydride under N_2 before used. Tetrahydrofuran (THF) and toluene were distilled over sodium under N_2 in the presence of benzophenone as the indicator prior to use.

Gel permeation chromatography (GPC) was conducted at 35 ^oC using a Shodex Sugar KS-802 column on an assembled instrument that was equipped with pump (Water Model-501), column oven, and refractive index detector (Schambeck SFD GmbH, RI-2000) connected in series. ^1H (400 MHz) and ^{13}C (100 MHz) NMR spectra were recorded on a Varian Mercury Plus 400 MHz spectrometer at room temperature using $CDCl_3$, DMSO-d_6, or D_2O as the solvent. Spectral processing (Fourier transform, peak assignment and integration) was performed using MestReNova 6.2.1 software. Matrix-assisted laser desorption ionization/time-of-flight mass spectrometry (MALDI-TOF-MS) was performed on a Bruker AutoFlex III TOF/TOF system in positive ion mode using either 2,5-dihydroxybenzoic acid (DHB) or α-cyano-4-hydroxycinnamic acid (CHCA) as the desorption matrix. Fourier-transform infrared (FT-IR) and Ultraviolet-visible (UV-Vis) absorption spectra were performed on a Bruker Alpha FT spectrometer and on a Thermo Genesys 10S UV-Vis spectrometer, respectively. Fluorescence spectroscopic analysis was carried out either on a Hitachi F-2500 spectrometer or on a Molecular Devices FlexStation 3 microplate reader at 25 ^oC.

Synthesis of PAMAM dendron G_1

A methanol solution (370 mL) of propargylamine (6.01 g, 0.109 mol) was added slowly into a methanol solution (110 mL) of methyl acrylate (28.1 g, 0.326 mol) under 0 ^oC. The reaction mixture was allowed to warm to room temperature and stirred for 3 days. The volatiles were removed under reduced pressure using a rotary evaporation to give half-generation dendron quantitatively. Then this compound (6.25 g, 27.5 mmol) dissolved in dry methanol (90 mL) was added dropwise into a methanol solution (370 mL) of EDA (66.1 g, 1.1 mol) under 0^{o}C over a period of 30 min. The reaction mixture was allowed to warm to room temperature and stirred for 3 days under a N_2 balloon until complete disappearance of terminal methyl ester groups. The solvent was removed under reduced pressure using a rotary evaporation, and excess EDA was carefully removed by azeotropic distillation at 35^{o}C using toluene and methanol mixture (9:1) to afford product **G_1** as a yellowish gum (30.0 g, 97%). ^1H NMR (400 MHz, $CDCl_3$): δ = 2.22 (t, J = 2.3 Hz, 1H), 2.38 (t, J = 5.8 Hz, 4H), 2.81-2.86 (m, 8H), 3.29 (dd, J = 11.6, 5.8 Hz, 4H), 3.43 (d, J = 2.3 Hz, 2H).

Synthesis of PAMAM dendron G_2

A methanol solution (40 mL) of **G_1** (3.44 g，12.1 mmol) was added slowly into a methanol solution (25 mL) of methyl acrylate (6.27 g，72.8 mmol) under 0^{o}C. The reaction mixture was allowed to warm to room temperature and stirred for 3 days. The volatiles were removed under reduced pressure using a rotary evaporation to give half-generation dendron quantitatively. This compound (6.39 g, 10.2 mmol) dissolved in dry methanol (35 mL) was added dropwise to a methanol solution (270 mL) of EDA (48.9 g, 0.814 mol) under 0^{o}C over a period of 30 min. The reaction mixture was allowed to warm to room temperature and stirred for 3 days under a N_2 balloon until complete disappearance of terminal methyl ester groups. The solvent was removed under reduced pressure using a rotary evaporation, and excess EDA was carefully removed by azeotropic distillation at 35^{o}C using toluene and methanol mixture (9:1) to afford product **G_2** as a yellowish gum (8.15 g, 91%). ^1H NMR (400 MHz, $CDCl_3$): δ = 2.22 (t, J = 2.3 Hz, 1H), 2.31-2.38 (m, 12H),

2.52 (t, J = 6.0 Hz, 4H), 2.74 (t, J = 6.0 Hz, 8H), 2.81 (t, J = 6.0 Hz, 12H), 3.22-3.31 (m, 12H), 3.44 (d, J = 2.3 Hz, 2H). MALDI-TOF-MS: Cacld. For $(M+H)^+$ $C_{33}H_{66}N_{13}O_6$: 740.5; Found: 740.6.

Boc-protection of PAMAM dendron G_1

A methanol solution (10 mL) of **G_1** (1.08 g, 3.81 mmol) was added slowly into a methanol solution (10 mL) of di-tert-butyl pyrocarbonate (2.50 g, 11.4 mmol) under -10 ^oC. The solution was stirred for 30 min and then allowed to warm to room temperature. After stirred for 4 h, the mixture was extracted with DCM (50 mL × 3); the combined organic phase was washed with brine (20 mL × 2) and dried over magnesium sulfate. After rotatory evaporation to dryness, repetitive precipitation in hexane afforded Boc-protected G_1 (**G_1-Boc**) as a yellowish solid (1.75 g, 95%). ^1H NMR (400 MHz, $CDCl_3$): δ = 1.44 (s, 18H), 2.22 (t, J = 2.3 Hz, 1H), 2.36 (t, J = 5.9 Hz, 4H), 2.82 (t, J = 5.9 Hz, 4H), 3.23-3.27 (m, 4H), 3.33-3.37 (m, 4H), 3.41 (d, J = 2.3 Hz, 2H), 5.41 (s, 2H).

Synthesis of (4-(azidomethyl)phenyl)methanol 1

A dry DCM solution (20 mL) of thionyl chloride (6.55 g, 55.1 mmol) in a dropping funnel was added dropwise into a dry DCM solution (40 mL) of p-xylylene glycol (6.90 g, 49.9 mmol) at 0 ^oC under nitrogen. The mixture was stirred at 0 ^oC for 1 h and then continued stirring under room temperature for an additional 20 h. The volatiles were removed under reduced pressure, and the residue was then extracted by DCM (50 mL × 3). After rotatory evaporation to dryness, further purification was carried out by flash column chromatography (SiO_2, ethyl acetate/hexane 2:3) to give (4-(chloromethyl)phenyl)methanol (5.15 g, 66%) as a colorless liquid. This compound (4.86 g, 31.0 mmol) dissolved in dry N,N-dimethylformamide (DMF, 60 mL) was then added dropwise into a DMF suspension of sodium azide (20.3 g, 0.310 mol) under nitrogen. The mixture was then stirred at 80 ^oC overnight. The organic solvent was removed under reduced pressure, and the residue was then extracted by ethyl acetate (50 mL × 2), followed by rotatory evaporation to give **1** as a colorless liquid (3.80 g, 75%). ^1H NMR (400 MHz, $CDCl_3$): δ = 2.60 (s, 1H), 4.30 (s, 2H), 4.62 (s, 2H).7.29 (d, J = 8.1 Hz, 2H), 7.33 (d, J = 8.1 Hz, 2H).

Synthesis of bis(4-(azidomethyl)benzyl) malonate 2

A dry DCM solution of dicyclohexylcarbodiimide (DCC, 6.95 g, 33.7 mmol) was added dropwise into a mixed dry DCM/THF (30:10 ml) solution of ***1*** (5.5 g, 33.7 mol), malonic acid (1.59 g, 15.3 mmol), and 1-hydroxybenzotriazole (HOBT, 695 mg, 10 wt% of DCC) under nitrogen at 0 ^oC. After 30 min, the mixture was then stirred under room temperature overnight. The reaction mixture was cooled to 0 ^oC to insure complete precipitation of the byproduct dicyclohexylurea (DCU), which is then quickly removed by vacuum filtration. After rotatory evaporation to dryness, further purification was carried out by flash column chromatography (SiO_2, ethyl acetate/hexane 2:3) to give **2** as a colorless liquid (3.50 g, 58%). ^1H NMR (400 MHz, $CDCl_3$): δ = 3.4

9 (s, 2H), 4.34 (s, 4H), 5.18 (s, 4H), 7.31 (d, J = 8.2 Hz, 4H), 7.34 (d, J = 8.2 Hz, 4H).

Synthesis of bis-azido-fullerene derivative 3

A dry toluene (350 mL) solution of C_{60} (350 mg, 0.486 mmol) was added with I_2 (148 mg, 0.583 mmol), **2** (201.3 mg, 0.510 mmol), and 1,8-diazabicycloundec-7-ene (DBU, 155 mg, 1.02 mmol) sequentially. The mixture was stirred under room temperature for 24 h. After rotatory evaporation to dryness, further

purification was carried out by flash column chromatography (SiO_2, DCM/hexane 7:3) to give **3** as a brown solid (270 mg, 50%). ^{1}H NMR (400 MHz, $CDCl_3$): δ = 4.36 (s, 4H), 5.48 (s, 4H), 7.34 (d, J = 8.4 Hz, 4H), 7.44 (d, J = 8.4 Hz, 4H).

Synthesis of $C_{60}G_1$ click cluster

A dry THF solution (30 mL) of **G_1-Boc** (246 mg, 0.509 mmol), **3** (270 mg, 0.242 mmol), and CuBr (73.2 mg, 0.510 mmol) was vigorously stirred under room temperature for 3 days and then quenched with aqueous ammonia. The organic solvent was removed using rotatory evaporation, and the residue was then extracted by ethyl acetate (50 mL × 2) to give Boc-protected **$C_{60}G_1$** as a dark brown solid. Carbamate deprotection is readily carried out by acid-promoted hydrolysis. Trifluoroacetic acid (TFA, 611 mg, 5.36 mmol) was added dropwise into a dry DCM solution (15 mL) of Boc-protected **$C_{60}G_1$** (226 mg, 0.109 mmol). The mixture was then stirred under room temperature for 2 days, and the volatiles were removed under reduced pressure. The mixture was washed with hexane repetitively to remove excess acid, and then freeze-drying afforded **$C_{60}G_1$** as a brown fluffy powder (207 mg, 89%). ^{1}H NMR (400 MHz, $CDCl_3$): δ = 2.82 (t, J = 6.4 Hz, 8H), 3.09 (t, J = 6.4 Hz, 8H), 3.47 (t, J = 6.4 Hz, 8H), 3.56 (t,J = 6.4 Hz, 8H), 4.14 (d, J = 2.0 Hz, 4H), 7.87 (s, 2H). MALDI-TOF-MS: Cacld. For $(M+H)^+$ $C_{105}H_{66}N_{16}O_8$: 1679.75; Found: 1680.46. Cacld. For $(M+Na)^+$ $C_{105}H_{66}N_{16}NaO_8$: 1702.74; Found: 1702.53.

Ethidium bromide displacement assay

0.5 mL of pEGFP-C1 solution (1 μg/mL) and 7 μL of EtBr solution (0.1 mg/mL) were mixed thoroughly in vials, followed by adding 8 μL of $C_{60}G_1$ solutions to achieve the desired N/P = 0.6, 0.8, 1.0, 1.2, and 2.0. Aliquots (200 μL) of thus-prepared solutions were then added into each well of 96-well black plates for the fluorescence measurement. 7 μL of EtBr (0.1 mg/mL) in ultrapure water (508 μL) was measured as the background fluorescence of EtBr, and the solution that only contains pEGFP-C1 and EtBr in 1:1 binding ratio corresponds to the N/P = 0 with maximum emission intensity. The fluorescence measurement was performed on Molecular Devices FlexStation 3 microplate reader using an excitation wavelength of 260 nm, and the emission spectra were recorded from 540 nm to 700 nm.

Characterization of complexe morphology, size, and ζ-potential

For atomic force microscopic (AFM) analysis, 5 μL of each sample was placed on a freshly cleaved mica sheet. After 5 min incubation at room temperature, the sheet was washed twice with 100 μL of double-distilled H_2O. The prepared samples were first dried from the edge of the mica sheet using a paper tissue, then by exposure to gentle air flow for 10 min. The samples were then immediately subjected to AFM study. We used a Nanoscope IIIa Multimode scanning probe microscope from Digital Instruments (Veeco Metrology Group, Santa Barbara, CA) in contacting mode with scan rate of 2.441 Hz and tip velocity of 2.35 μm/s. Analyses of the images were carried out using the Nanoscope III software version 5.31R1. Dynamic light scattering (DLS) and ζ-potential measurements were performed on Malvern Zetasizer Nano series. Transmission electron microscopy (TEM) images were taken by a Hitachi H-7000 electron microscope with Hamamatsu C4742-95 digital camera operated at an accelerating voltage of 100 kV.

Cellular uptake of the $C_{60}G_1$/DNA complexes

HeLa cells and MCF-7 cells were obtained from the American Type Culture Collection (ATCC,

Manassas, VA). MCF-7 cells were cultured in MEMα medium (Life Technologies Corporation) supplemented with 10% fetal bovine serum (Hyclone), bovine insulin (5 μg/mL, Sigma-Aldrich), sodium pyruvate (1 mM, Biological Industries), antibiotics (100 U/ml penicillin and 100 μg/mL streptomycin, Life Technologies Corporation) and Glutamax (2 mM, Life Technologies Corporation). HeLa cells were cultured in DMEM medium (Life Technologies Corporation) with supplements as used for MCF-7 cultivation except for bovine insulin. The cells were maintained in a 5% CO_2 air humidified atmosphere at 37 °C.

To evaluate the cellular uptake efficiency of the $C_{60}G_1$/DNA complex, pEGFP-C1 (Clontech) was labeled with YOYO-1 fluorescent dye (Life Technologies Corporation). Briefly, 500 μL of pEGFP-C1 solution in water (1 μg/mL) was mixed with 4 μL of 200 μM YOYO-1 and incubated at room temperature for 10 min. Then, 3.2 μL of $C_{60}G_1$ (0.5 μg/μL) and TurboFect (Fermentas, Thermo Scientific, Pittsburgh PA, USA) containing YOYO-1-labeled plasmid DNA were added to the cells with the complete medium (DMEM with 10 % FBS and antibiotics), and further cultured for 2 h before being harvested for fluorescence microscope and flow cytometric analysis.

In vitro gene transfection

Prior to transfection, cells were seeded in 12-well plate at a density of 1.2×10^5 cells per well, in 0.5 ml complete medium (DMEM with 10 % FBS and antibiotics). After incubation for 24 h, the culture medium was changed to the medium containing $C_{60}G_1$/DNA complex solutions (0.5 mL/well) which were prepared as follow: 449 μL of $C_{60}G_1$ solution, ranging from 1.6 to 51.8 μg/mL, was mixed thoroughly in water with 1 μL of pEGFP-C1 solution (0.5 μg/μL). The mixtures with a total volume of 450 μL were agitated thoroughly to result in electrostatic complexes with specific N/P ratios of 1, 2, 4, 8, 16, 32, where the final concentration of $C_{60}G_1$ equals 0.75 to 24.3 μM. The prepared solutions incubated at room temperature for 3 h were mixed with 50 μL of serum-containing medium (100 % FBS) and then added into the respective dishes of cells. After incubation at 37°C for another 6 h, the transfection medium was replaced with the complete medium and cultured for another 48 h before being harvested for fluorescence microscope, flow cytometry, and Western blot analysis.

Fluorescence microscopy and flow cytometry

For observation of GFP+ cells, cells were observed for green fluorescence signals with inverted fluorescent microcopy (Axioskop 2, ZEISS, Germany) with 100 W halogen lamp, 480/30 nm band-pass blue excitation filter, a 505 nm dichroic mirror, and a 535/40 nm band-pass barrier filter. Images were captured with cool CCD camera and processed with MetaMorph Software (Molecular Devices). For quantification with GFP+ cells, cells were harvested with trypsin/EDTA, resuspended in 200 μl of PBS/1 % bovine serum albumin (Sigma-Aldrich), and analyzed by flow cytometry (Epics XL, Beckman Coulter). The green fluorescence emission (525 nm) illuminated with 488nm blue laser and signals were collected with software provided by the manufacture. The percentage and mean fluorescence intensity of GFP+ cells were further analyzed by WinMDI software (The Scripps Research Institute, San Diego, USA). Each data shown in Fig. 9 was expressed as mean ± standard deviation of three experiments.

Western blotting analysis

The cells were harvested following the transfection protocol described above. To prepare the whole-cell extract, cells were lysed in a lysis buffer solution (pH = 7.5) containing 50 mM Tris, 5 mM EDTA, 150 mM

NaCl, 1 % NP40, 0.5 % deoxycholic acid, 1 mM sodium orthovanadate, 81 μg/mL aprotinine, 170 mg/mL leupeptin, and 100 mg/mL PMSF. After incubation at 4 °C for 30 min, the mixtures were centrifuged at 10,000 g for 10 min, and the supernatants were collected as whole-cell extracts. The protein concentration of the whole cell extracts was determined by BCA protein assay reagent (Pierce). Twenty-five micrograms of whole cell extracts were then separated by 8-12 % SDS-PAGE and transferred onto PVDF membrane (Millipore). After blocking with 5 % non-fat milk, the membrane was incubated with mouse anti-GFP antibody (1:1000 dilution, Santa Cruz Biotechnology Inc.) at 4 °C overnight, then washed with 0.1 % Tween-20/PBS solution. The membrane was then incubated with peroxidase-conjugated anti-mouse IgG antibody (1:10000 dilution, Perkin-Elmer) at room temperature for 1 h followed by washing with 0.1 % Tween-20/PBS for 3 times. The signals were detected by enhanced chemiluminescence substrate (Perkin-Elmer) and captured with a chemiluminescence recorder (ImageQuant™ LAS 4000 mini, GE Healthcare Life Science).

Agarose gel electrophoresis analysis of complexing capacity between $C_{60}G_1$ and DNA.

0.5 μg of pEGFP-C1 palsmid DNA was dissolved in nuclease-free H_2O and $C_{60}G_1$ was then added at different N/P ratio (range from 0.5 to 2.0) to final volume of 15 μl. After mixing well and incubating at room temperature for 30 min, the $C_{60}G_1$/DNA solutions were added with 3 μl of Novel juice DNA loading dye (GeneDirex), loaded into wells of 1.0 % agarose gel, and performed electrophoresis in TAE buffer (40 mM Tris-acetate, 1 mM Na_2-EDTA, pH = 8.5) at 150 V for 1 h. DNA signals were detected by SafeBlue Imager System (Major Science, Saratoga, CA, USA) with a blue light LED source to visualize the DNA bands and images were captured by a digital camera (Canon G15, Ohta-ku, Tokyo, Japan). The intensities of DNA bands were analyzed by ImageJ software (NIH, Bethesda. MA, USA).

Results and discussion

Material Synthesis and Characterization

Our strategy for the synthesis of amphiphilic C_{60}-PAMAM-dendron click clusters comprised 2 parts. (1) The preparation of a counterpart: the NH_2-terminated PAMAM dendron was prepared by a divergent pathway using propargylamine as the focal point. As shown in Fig. 1, a conventional 2-step procedure consisting of a Michael addition followed by amidation produces the G_1 PAMAM dendron. All NH_2 terminals were then protected with Boc groups to prevent unwanted complexation with the copper catalysts; (2) as shown in Fig. 2, the diazido-functionalized fullerene derivative was prepared in high yield by a Bingel reaction. The conjugation of the as-prepared PAMAM dendrons and the C_{60} derivative was conducted through a copper(I)-catalyzed azide-alkyne cycloaddition (CuAAC "click" reaction) to produce the protected click clusters. Finally, acidic hydrolysis was performed to deprotect the amino groups, and produce the highly water-soluble amphiphilic C_{60} and G_1 PAMAM dendron conjugate, namely $C_{60}G_1$.

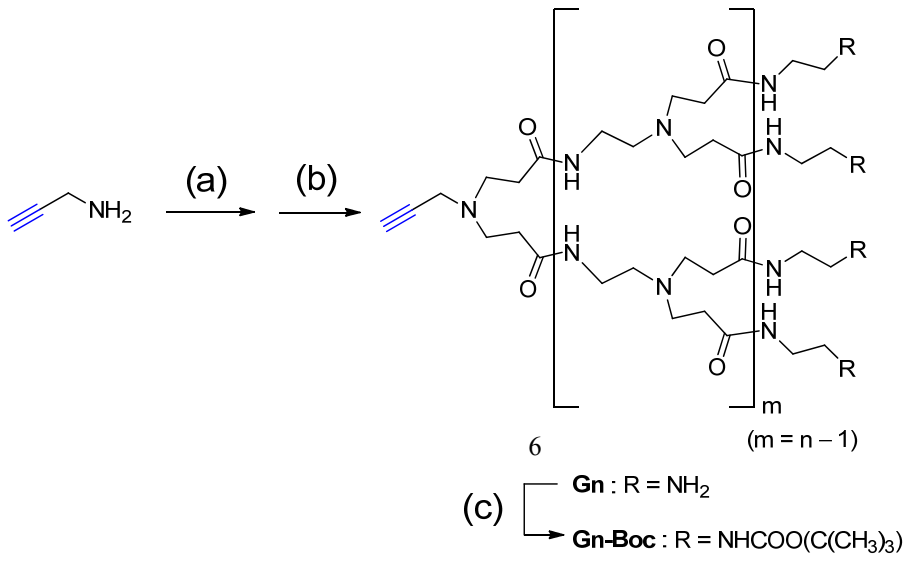

Fig. 1 Synthesis of $\mathbf{G_1}$ and $\mathbf{G_2}$ PAMAM dendrons bearing a propargyl focal point. (a) methyl acrylate, methanol; (b) EDA, methanol; (c) di-tert-butyl pyrocarbonate, methanol.

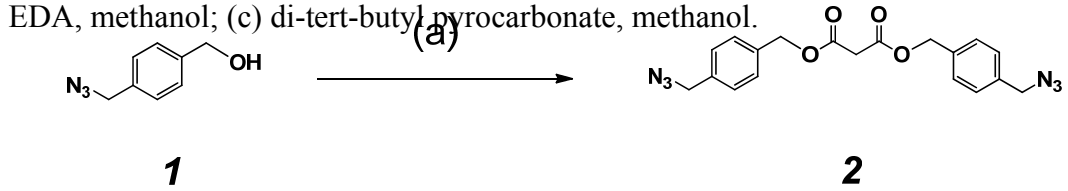

1 *2*

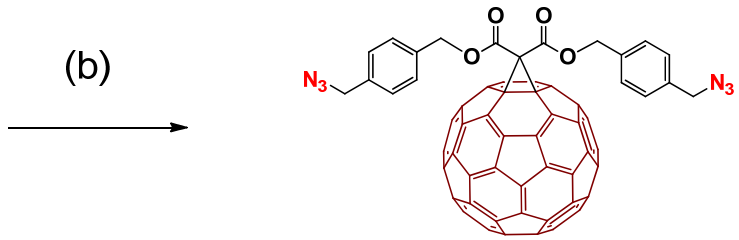

3

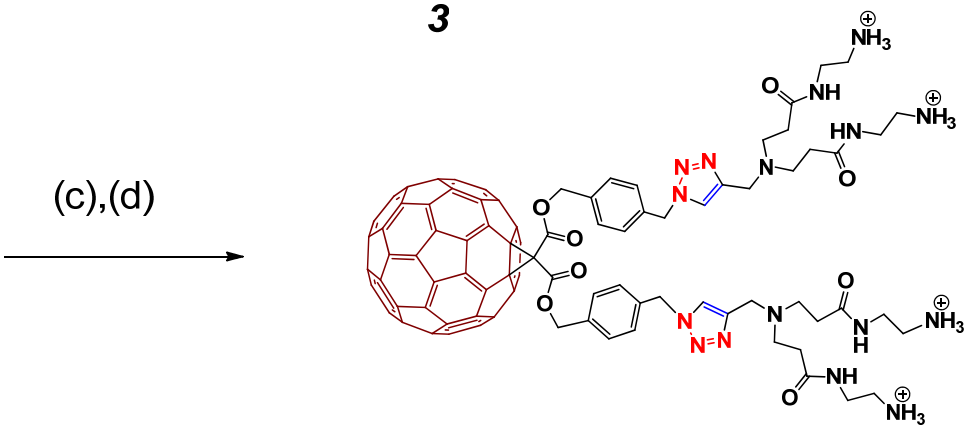

$C_{60}G_1$

Fig. 2 Synthesis of amphiphilic PAMAM dendron-bearing C_{60} click cluster ($\mathbf{C_{60}G_1}$). (a) malonic acid, DCC, HOBT, THF/CH_2Cl_2, 0 °C to room temperature; (b) C_{60}, DBU, I_2, toluene; (c) $\mathbf{G_1}$**-Boc**, CuBr, THF; (d) TFA, CH_2Cl_2.

$C_{60}G_1$ and its precursors were fully-characterized by ^{1}H NMR, FT-IR, UV-Vis spectroscopy, gel permeation chromatography (GPC), and MALDI-TOF mass spectrometry. The ^{1}H and ^{13}C NMR spectra of compounds **2** and **3** (Fig. S1 and S2) clearly indicate the successful synthesis of a Bingel adduct with diazido groups, by the disappearance of the malonate center protons at 3.5 ppm. Notably, although the azido group could attack the fullerene moiety to cause cycloaddition, compound **2** was stable in dilute solution. FT-IR spectroscopy confirmed the success of the click coupling between the Boc-protected G_1 PAMAM dendron and the diazido fullerene, by the disappearance of the azide stretching band at 2094 cm^{-1} (Fig. 3a), and by the appearance of characteristic proton and carbon resonances of the click counterpart in the ^{1}H NMR spectra (Fig. S3). Finally, complete deprotection of the Boc groups was confirmed by the disappearance of the corresponding protons at 1.5 ppm from the ^{1}H NMR spectrum, supporting the formation of the highly water-soluble cationic C_{60} derivative bearing two NH_2-terminated G_1 PAMAM dendrons (Fig. 3b). Additionally, the appearance of the triazole proton resonance at 7.9 ppm suggests that CuAAC click coupling was successful, indicating the exclusive formation of the 1,4-regioisomer.[29] Moreover, UV-Vis analysis of the as-prepared click clusters (Fig. 3c) show a broad absorption maximum at approximately 330 nm, clearly indicating the existence of a fullerene core. Aqueous phase GPC combined with cationic exchange

chromatography (Fig. 3d) revealed monodispersed elution peaks for $C_{60}G_1$, confirming that the click reaction produced a single product in high purity. MALDI-TOF mass spectrometry results support our proposed structure by demonstrating an exact match between calculated and observed molar masses for the $C_{60}G_1$ click cluster (Fig. 3e).

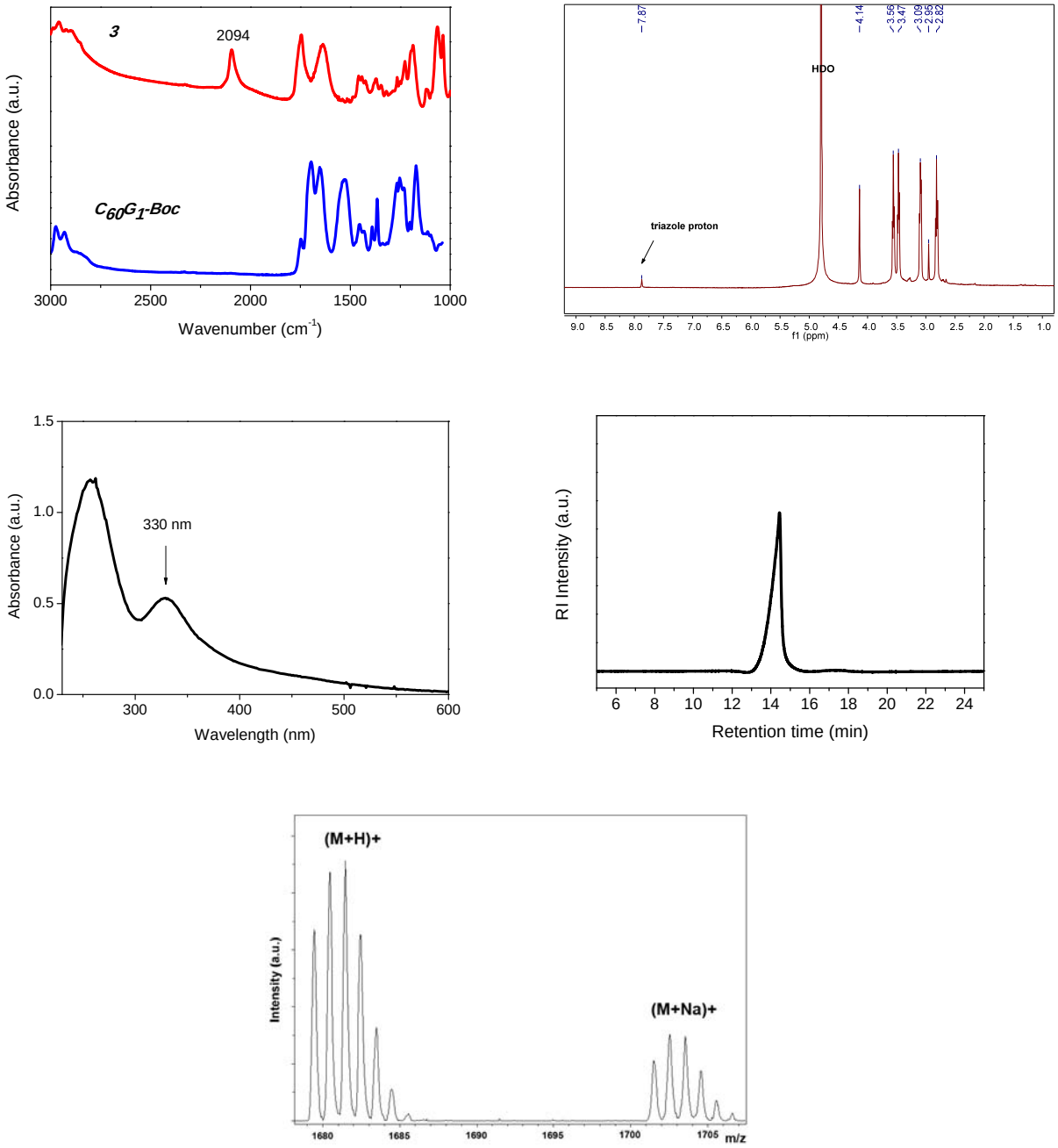

Fig. 3 (a) FT-IR spectra of **3** and Boc-protected $\mathbf{C_{60}G_1}$. (b) ^{1}H NMR spectrum, (c) UV-Vis spectrum, (d) GPC chromatogram, and (e) MALDI-TOF-MS spectrum of $\mathbf{C_{60}G_1}$.

Self-Aggregation of Amphiphilic $C_{60}G_1$ and DNA Complexes

Because of its amphiphilic nature, $C_{60}G_1$ assembles into core-shell-like micelles rather than remaining in a single molecular form in aqueous media.[30] Therefore, we used AFM to analyze the $C_{60}G_1$self-aggregation behavior. Fig. 4a shows microscopic images of $C_{60}G_1$ deposited on a freshly cleaved mica surface, clearly confirming the formation of nanoclusters, with an average dimension of 22.4 ± 3.7 nm. The results of dynamic light scattering (DLS) experiments were in agreement with the AFM results, indicating comparable dimensions for these micelle-like nanoparticles, with a *z*-average size distribution of 24.8 ± 0.2 nm, and a

polydispersity index of 0.255 ± 0.008. Both sets of data are consistent with the magnitude of primary micelles comprising a hydrophobic C_{60} core and hydrophilic PAMAM dendron shell. Moreover, TEM analysis demonstrated a micelle-like structure with sharp contrast between the core and shell components (Fig. 4b).

Recently, López et al. reported a series of regio-isomeric dendron-fulleropyrrolidines with no aggregation occurring up to 10^{-3} mol L^{-1}.[31] However, on the basis of AFM and DLS analysis, we found that the $C_{60}G_1$ favors the formation of nanoparticles at much lower concentration of approximately 5×10^{-6} mol L^{-1}. Thus, C_{60} could serve as a hydrophobic building block, and so drive PAMAM dendron assembly to form a "pseudodendrimer". Moreover, zeta-potential measurement further indicated that these C_{60}-centered pseudodendrimers carry multiple positive charges on their surfaces (22.3 ± 5.2 mV), allowing electrostatic interactions with polyanionic targets such as plasmid DNA.

We evaluated the binding affinity of amphiphilic $C_{60}G_1$ towards pEGFP-C1 (4731 base pairs) using an ethidium bromide (EtBr) displacement assay.[32] The DNA intercalating agent EtBr is commonly used in molecular biology to detect nucleic acids. The competition for binding with DNA, between EtBr reagents and polyamine-based vectors towards DNA, allows us to determine the minimum N/P ratio necessary for effective complexation. In the assay, the optimized N/P ratio is expressed as a 50% charge excess (CE_{50}) value, which represents the "excess charge" on the cationic vector relative to anionic DNA that is required for 50% EtBr displacement. A lower CE_{50} value, provided by a smaller N/P ratio, represents more effective binding of the 2 components. Fig. 5a provides fluorescence titration data for the addition of $C_{60}G_1$, where the maximum fluorescence intensity corresponds to the 1:1 binding of EtBr and a DNA base in the absence of $C_{60}G_1$, and the minimum intensity corresponds to the amount of free EtBr in water. We attributed the enhanced and blue-shifted emission pattern arising from the intercalating complex to the less polar environment inside the DNA helix. Emission intensity continually decreased with increasing $C_{60}G_1$ concentration, suggesting that intercalating EtBr molecules were gradually displaced by C_{60}-based vectors. The CE_{50} value calculated from the linear correlation of relative fluorescence intensities at 605 nm versus the charge excess values (CE) was found to be only 1.3 (Fig. 5b), clearly confirming that amphiphilic $C_{60}G_1$ is an effective DNA binder. Barnard et al. demonstrated the effective DNA binding of a family of amphiphilic dendrons bearing either long alkyl chains or cholesterols as the hydrophobic building blocks.[33] The authors reported that self-assembled dendrons consistently achieved superior EtBr displacement, and had lower CE_{50} values, compared to non-self-assembled complexes. In our study, we found that a net positive charge of +4 per $C_{60}G_1$ molecule was insufficient to displace more than 50% of EtBr from its intercalation sites. However, the strong interaction of the hydrophobic C_{60} moiety is capable of inducing the close-packing of positively charged dendrons to form a C_{60}-based pseudodendrimer, by which DNA could be more efficiently wrapped into compact electrostatic complexes of a size that is suitable for cellular uptake. Additionally, gel electrophoresis analysis confirmed strong binding between $C_{60}G_1$ and DNA; more than 90% of DNA bound to C_{60}-based vectors at N/P ratios greater than 1.2 (Fig. 5c), consistent with our spectroscopic results.

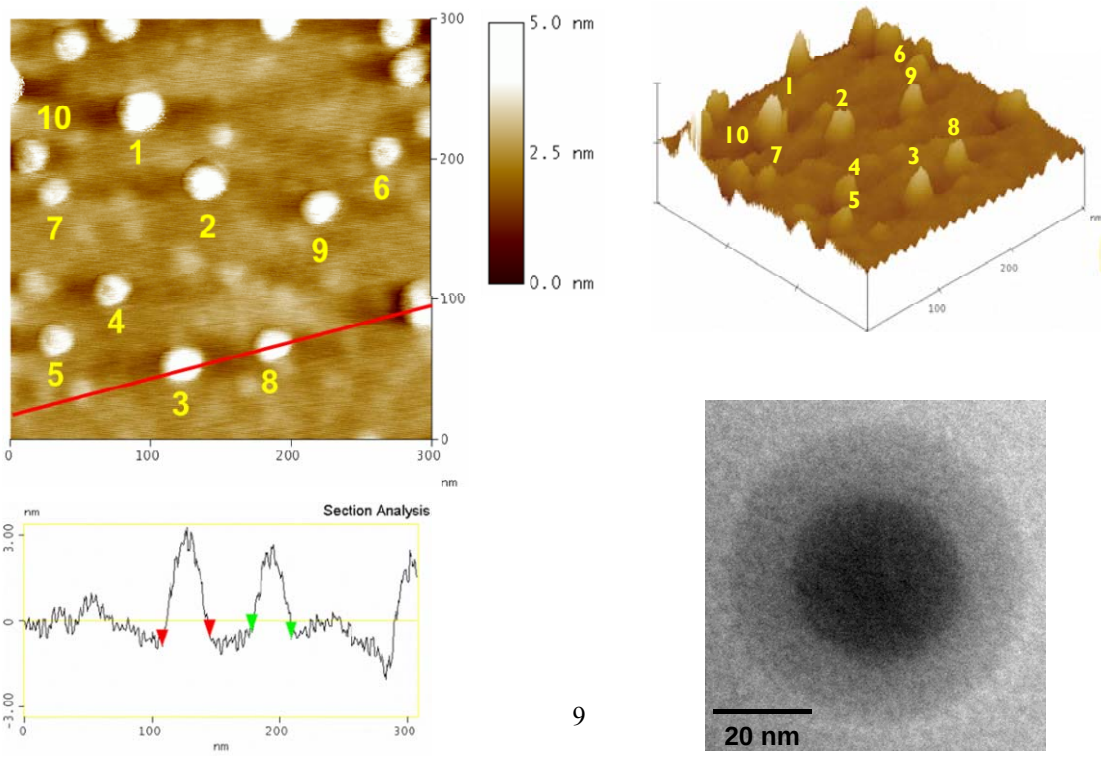

Fig. 4 (a) AFM micrograph and section analysis for $\mathbf{C_{60}G_1}$ aggregates on mica surface. The particle dimension averaged by 10 selected particles is 22.4 ± 3.7 nm. (b) TEM micrograph of core-shell-like $\mathbf{C_{60}G_1}$ aggregates.

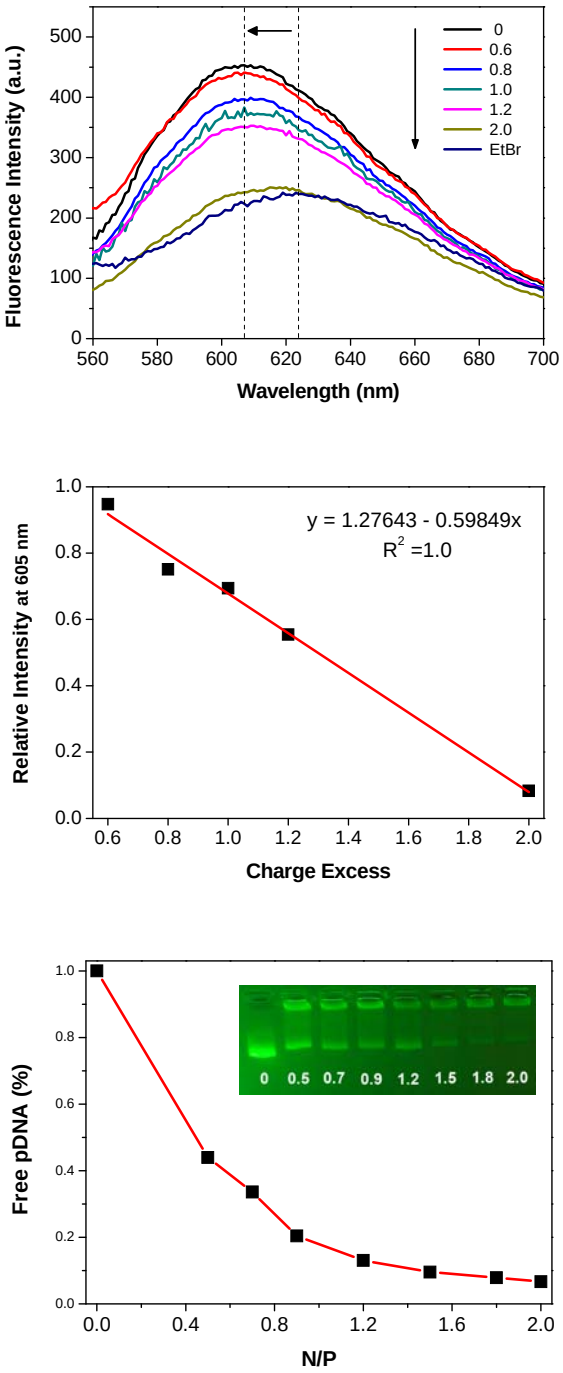

Fig. 5 (a) Fluorescence titration data for the addition of $\mathbf{C_{60}G_1}$ to DNA at various nitrogen-to-phosphorous (N/P) ratios. The maximum fluorescence intensity corresponds to the 1:1 binding of EtBr and a DNA base in the absence of $\mathbf{C_{60}G_1}$, and the minimum intensity corresponds to the amount of free EtBr in water. (b) The

linear correlation of relative fluorescence intensities at 605 nm versus the charge excess values. (c) Agarose gel electrophoresis analysis for determining the optimized binding capacity of **$C_{60}G_1$** at various N/P ratios.

AFM scanning was used to further visualize the morphology of the $C_{60}G_1$ and DNA complex at an optimized ratio of N/P = 2 to ensure complete binding between the vector and nucleic acids. Fig. 6 shows micrographs of the as-formed complexes on a 2 × 2 μm mica surface, confirming the electrostatic condensation of $C_{60}G_1$ with DNA, and clearly indicating a dynamic formation process. The small white dots in Fig. 6a represent uniformly dispersed $C_{60}G_1$ nanoclusters; Fig. 6b shows their partial aggregation into larger particles 30 min after mixing with pEGFP-C1 in water. At this stage, free $C_{60}G_1$ self-aggregates predominated over the DNA complexes, however, after standing for 3 h, the mixing solution exclusively contained the electrostatic DNA complexes, with an average diameter of approximately 140 nm, as determined by AFM section analysis (Fig. 6c). DLS measurements also verified the dynamic formation process by revealing an increasing particle size distribution and narrowing polydispersity index, from 93 nm and 0.37, to 110 nm and 0.29, respectively. An optimized N/P ratio is a critical factor in DNA complex formation using polyamine-based vectors. Both AFM and DLS analyses suggested that extended complexation time benefit the formation of DNA/$C_{60}G_1$ hybrid nanoparticles with favorable dimensions for cellular uptake.

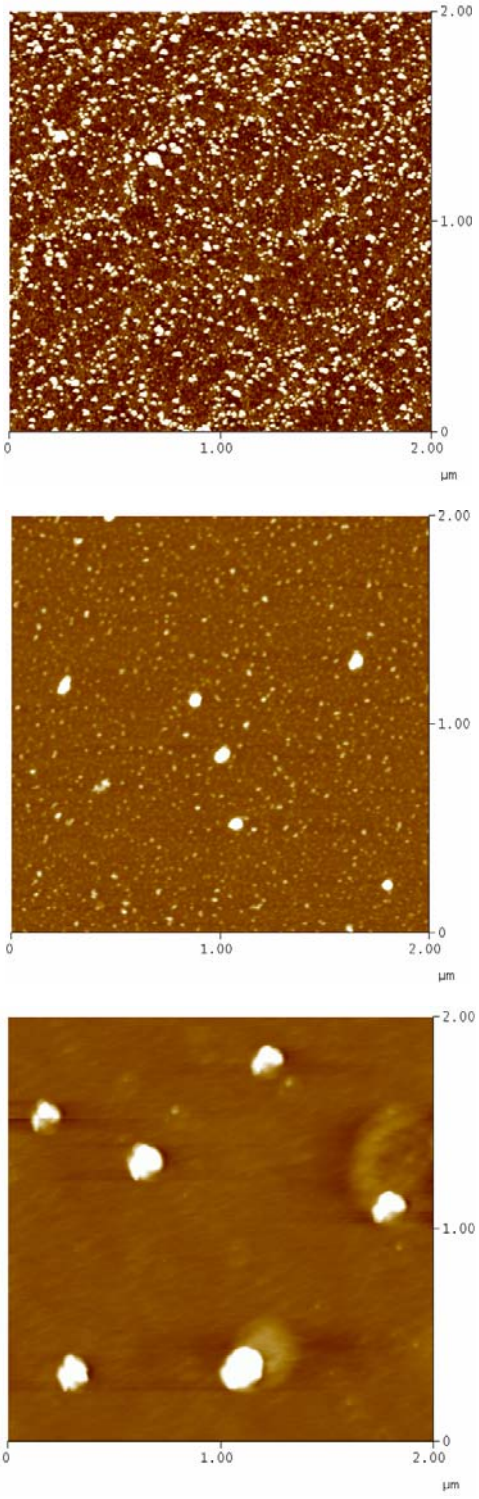

Fig. 6 AFM micrographs of initial $\mathbf{C_{60}G_1}$ (4.7×10^{-6} mol L^{-1}) on 2 × 2 μm mica surface (a), mixing DNA with $\mathbf{C_{60}G_1}$ at N/P = 2 for 30 min (b), and 180 min (c).

Gene Delivery into HeLa and MCF-7 Cell lines

We performed a cellular uptake study using fluorescent YOYO-1 cyanine-based probes, which readily intercalate DNA with high binding affinity.[34] YOYO-1 does not emit fluorescence until bound to double-stranded DNA, when the emission intensity for these complexes dramatically increases (Fig. S4). The fluorescence enhancement observed during the cellular uptake experiment confirmed the uptake of YOYO-1 labeled DNA, and allowed us to trace the in vitro and in vivo biodistributions of nucleic acids. To evaluate $C_{60}G_1$–mediated gene delivery, pEGFP-C1 was pretreated with YOYO-1, followed by mixing with $C_{60}G_1$ at an N/P ratio of 2, to ensure complete association between DNA, vectors, and probe molecules. A commercially available transfection reagent (TurboFect) was used as a positive control for 2 cell lines - a breast cancer cell line, MCF-7 and a cervical cancer cell line, HeLa. Fluorescent microscopic images clearly show that the $C_{60}G_1$/DNA complexes are taken up by both MCF-7 and HeLa cells (Fig. 7).

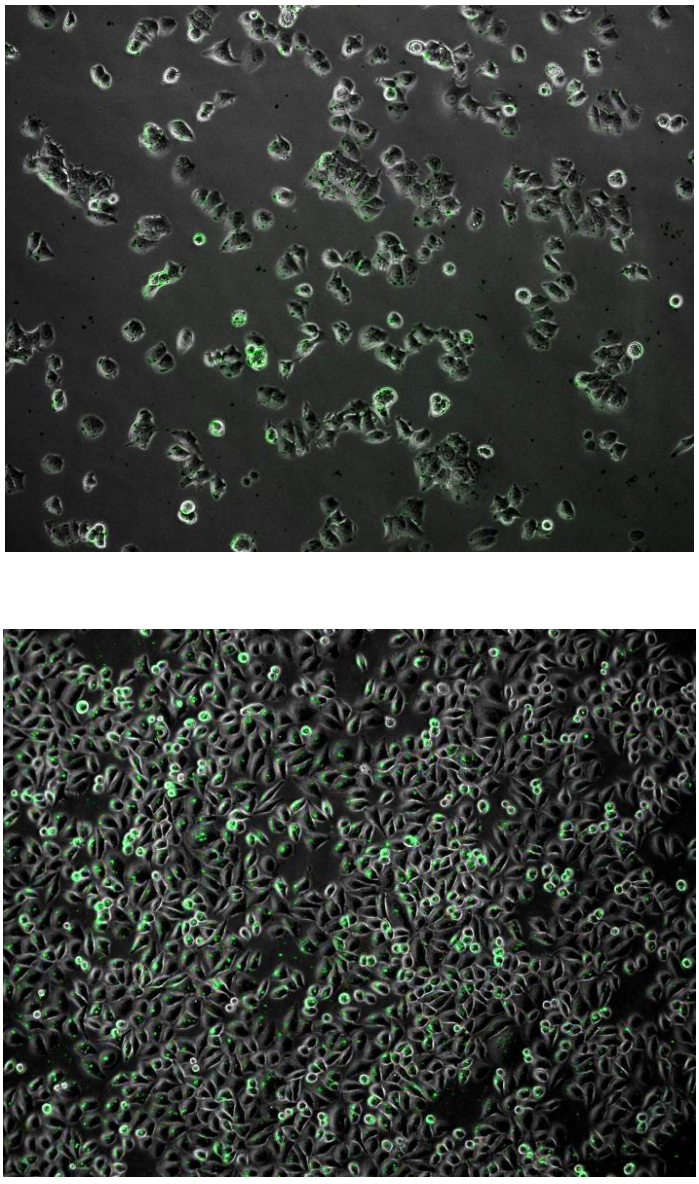

Fig. 7 The overlaying optical and fluorescence microscope images for (a) MCF-7 and (b) HeLa cell lines internalized by $\mathbf{C_{60}G_1}$/DNA complexes at N/P = 2. The green spots represent a successful cellular uptake of

YOYO-1-labeled DNA.

Flow cytometry analysis was performed to quantify the MCF-7 and HeLa cellular uptake efficiencies of $C_{60}G_1$/DNA. Because the self-penetrating behavior of fluorescence dyes may affect the counting of positive cells, we used cells transfected by YOYO-1 alone as the negative control for the flow cytometry analysis. Notably, the result revealed YOYO-1 self-penetration into the target cell lines without the aid of a vector; and approximately 59% of HeLa cells were YOYO-1 positive, with weak mean fluorescence intensity of 48 units (Fig. S5). The flow histograms shown in Fig. 8 indicate that the complex could be taken up by both MCF-7 and HeLa cells, in agreement with the microscopic results. Fig. 9 lists quantitative data in terms of the positive cells, and the mean fluorescence intensities for cells transfected by YOYO-1, DNA/YOYO-1 (Fig. 9a), $C_{60}G_1$/YOYO-1 (Fig. 9b), TurboFect/DNA/YOYO-1 (Fig. 9c), and $C_{60}G_1$/DNA/YOYO-1 complexes (Fig. 9d). Comparing the 2 cell lines, we found that at an N/P ratio of 2, the overall uptake efficiency of $C_{60}G_1$/DNA complexes towards HeLa cells was slightly greater than that for MCF-7 cells. Approximately 51% of HeLa cells were internalized by the $C_{60}G_1$/DNA complexes, where the mean fluorescence intensity was 371 units, and approximately 43% of MCF-7 cells were positive to the complexes, with a mean fluorescence intensity of 570 units. These results suggest that using $C_{60}G_1$ assembly as a DNA vehicle is comparable to the TurboFect–mediated delivery system. We also performed a control experiment using amine-terminated G_2 PAMAM Dendron as the gene vector, and no cellular uptake was observed at the N/P value of 2 (Fig. S6). The G_2 dendron bears the same number of surface charges as $C_{60}G_1$, but lacks sufficient self-aggregation to deliver DNA into the target cells. Thus, the amphiphilic structure of $C_{60}G_1$ is crucial for gene delivery. Moreover, while comparing Fig. 9a and 9b, we found that approximately 3% of cells were internalized by YOYO-1 with remarkable fluorescence enhancement in the presence $C_{60}G_1$ (465 units for MCF-7 cells and 362 units for HeLa cells). Although the mechanism is unclear, we speculated that $C_{60}G_1$ is also capable of delivering rigid aromatic compounds into target cells.

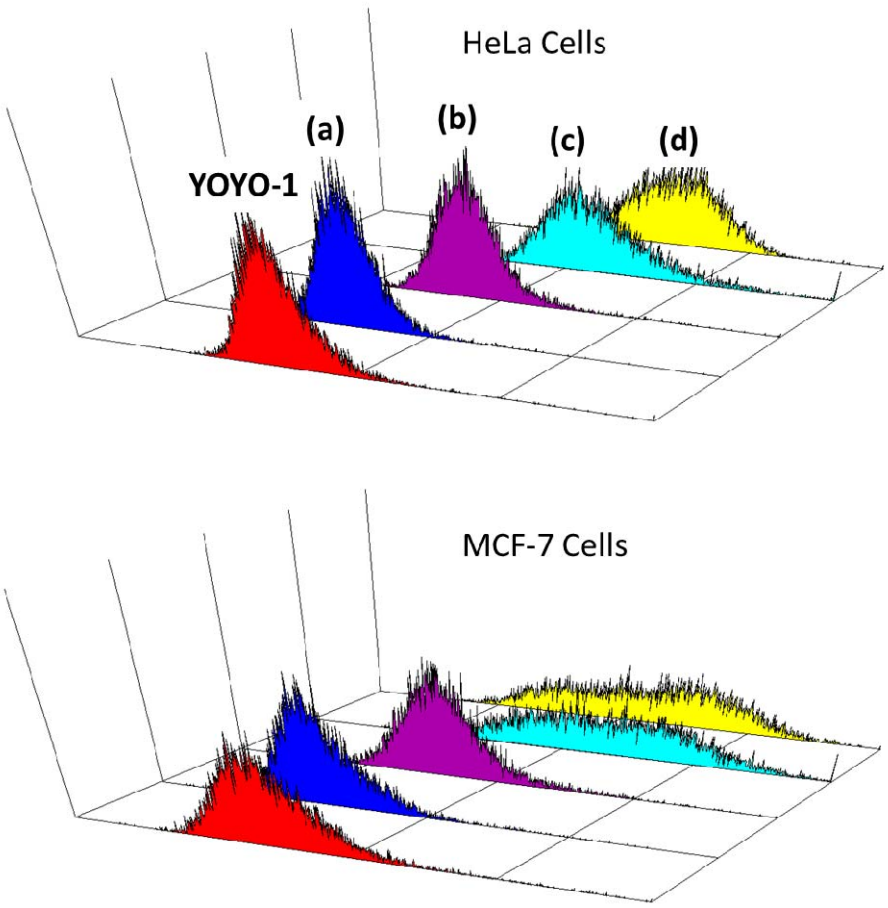

Fig. 8 The flow cytometry histograms for counting 1×10^4 cells internalized by (a) DNA/YOYO-1, (b) **$C_{60}G_1$**/YOYO-1, (c) TurboFect/DNA/YOYO-1, and (d) **$C_{60}G_1$**/DNA/YOYO-1 complexes at N/P = 2. The incident laser wavelength was set to 488 nm.

After confirming successful cellular uptake at an N/P ratio of 2, we performed in vitro gene transfection of $C_{60}G_1$/DNA complexes into MCF-7 cells. The main obstacle for this process was the limited endosomal release of pEGFP-C1, required for the expression of enhanced green fluorescence proteins (EGFP). The transfection efficiency for both cell lines, as determined by fluorescence techniques or by Western blotting, was extremely low at this N/P ratio. No effective transfection was observed with increasing N/P ratio, until N/P = 32. GFP expression, monitored by fluorescence microscope and Western blot analysis (Fig. 10), revealed approximately 50% EGFP expression at N/P = 32 relative to TurboFect-mediated delivery. Although the preliminary results obtained using $C_{60}G_1$ as gene vector do not guarantee that high uptake efficiency should result in high gene transfection, $C_{60}G_1$ is capable of delivering plasmid DNA into target cells with moderate transfection efficacy at high N/P values. In this regard, we speculate that a strong binding between $C_{60}G_1$ and DNA might disfavor endosomal escape of genes, and thus incorporation of flexible, or pH and light stimuli-responsive building blocks into the amphiphilic dendritic structures should enhance the overall transfection efficiency at lower N/P ratios. Investigations along this line are now underway and will be reported in due course.

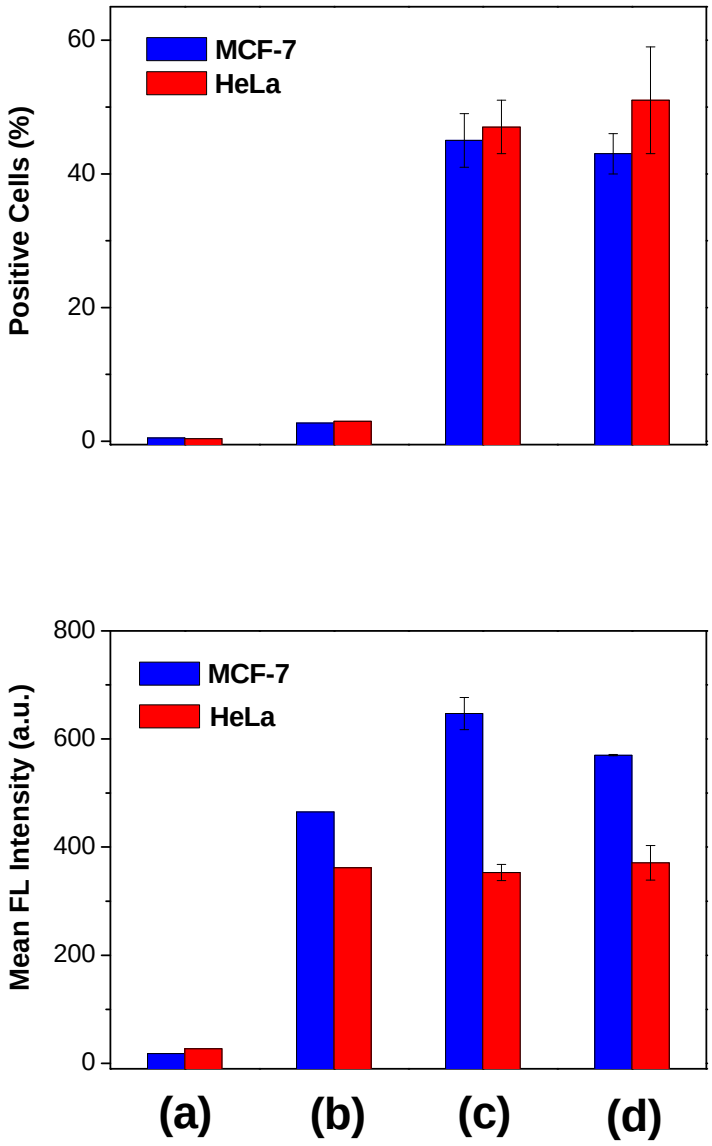

Fig. 9 The quantitative analysis for flow cytometry in terms of positive cells and mean fluorescence intensity for cells internalized by (a) DNA/YOYO-1, (b) **$C_{60}G_1$**/YOYO-1, (c) TurboFect/DNA/YOYO-1, and (d) **$C_{60}G_1$**/DNA/YOYO-1 complexes at N/P = 2, , where the concentrations of **$C_{60}G_1$**, DNA bases, and YOYO-1 are 1.51, 3.03, and 1.60×10^{-6} mol L^{-1}, respectively.

Conclusions

Using a "pseudodendrimer" composed of amphiphilic dendrons as a non-viral gene vector, we developed a simple synthesis for a NH_2-terminated PAMAM dendron-bearing fullerenyl dyad through the CuAAC click reaction. The amphiphilic structure and solvophobic nature of C_{60} induce the dyad to form uniform core-shell-like nanoparticles in water. The polycationic C_{60}-based nanoparticles bind firmly with negatively charged pDNA at low N/P ratios, and both HeLa and MCF-7 cell lines readily take up the resulting electrostatic complexes. As with Turbofect-mediated gene transfection, this system also shows moderate in vitro EGFP expression at higher N/P ratios. Although the binding affinity and cellular uptake obtained using C_{60}-based nanoparticles as carrier are favorable, a strong interaction between the vector and pDNA may decrease endosomal release rates, which, in turn may down-regulate the final protein expression. Thus, we anticipate that this system could be improved by incorporation of acid- or photo-labile functional moieties between the hydrophilic PAMAM dendron and the hydrophobic C_{60}, to control gene release by pH- or light-stimulation. Moreover, comparing with the amphiphilic dendrons using long alkyl chains or cholesterol as hydrophobic counterpart, we also anticipate that the C_{60}-based dendrons may combine the multiple functions of gene transfection, antioxidants, and photosensitizers into a single gene vehicle for biological applications.

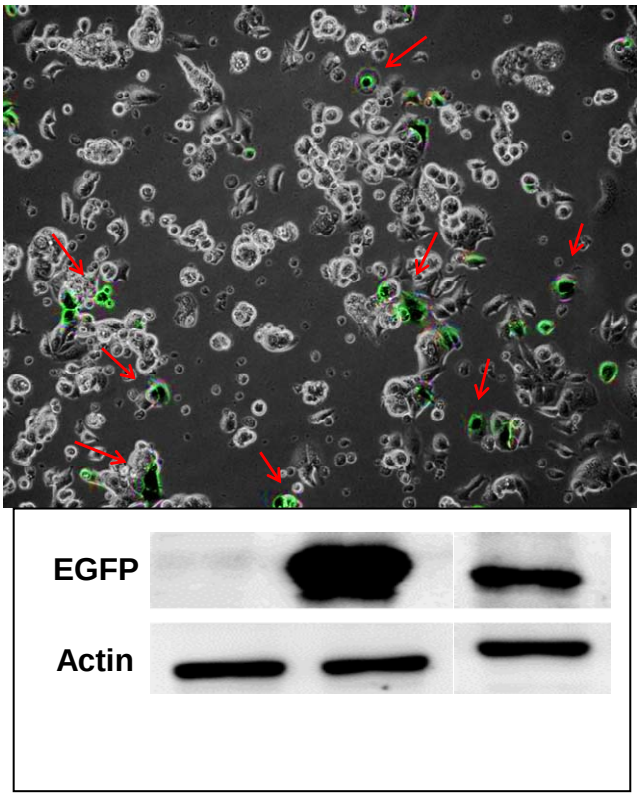

Fig. 10 In vitro gene transfection with the EGFP expression monitored by overlaying optical and fluorescence microscope images and Western blotting analysis. (a) DNA only (negative control), (b) TurboFect/DNA (positive control), and (c) $\mathbf{C_{60}G_1}$/DNA at N/P = 32, approximately 50% EGFP expression relative to TurboFect-mediated delivery.

Notes and references

1 M. X. Tang, C. T. Redemann and F. C. Szoka, *Bioconjugate Chem.,* 1996, **7**, 703-14.

2 G. Navarro and C. Tros de Ilarduya, *Nanomedicine*, 2009, **5**, 287-97.

3 V. K. Yellepeddi, A. Kumar and S. Palakurthi, *Anticancer Res.*, 2009, **29**, 2933-43.
4 R. Esfand and D. A. Tomalia, *Drug Discovery Today*, 2001, **6**, 427-36.
5 V. Russ, H. Elfberg, C. Thoma, J. Kloeckner, M. Ogris and E. Wagner, *Gene Ther*., 2008, **15**, 18-29.
6 J. L. Santos, H. Oliveira, D. Pandita, J. Rodrigues, A. P. Pêgo, P. L. Granja and H. Tomás, *J Controlled Release*, 2010, **144**, 55-64.
7 E. Yuba, Y. Nakajima, K. Tsukamoto, S. Iwashita, C. Kojima, A. Harada and K. Kono, *J Controlled Release*, 2012, **160**, 552-60.
8 T. Yu, X. Liu, A. L. Bolcato-Bellemin, Y. Wang, C. Liu, P. Erbacher, F, Qu, P. Rocchi, J. P. Behr and L. Peng, *Angew. Chem. Int. Ed*., 2012, **51**, 8478-84.
9 M. Guillot-Nieckowski, D. Joester, M. Stöhr, M. Losson, M. Adrian, B. Wagner, M. Kansy, H. Heinzelmann, R. Pugin, F. Diederich and J. L. Gallani, *Langmuir*, 2006, **23**, 737-46.
10 T. Takahashi, K. Kono, T. Itoh, N. Emi and T. Takagishi, *Bioconjugate Chem.*, 2003, **14**, 764-73.
11 M. Guillot, S. Eisler, K. Weller, H. P. Merkle, J. L. Gallani and F. Diederich, *Org. Biomol. Chem*., 2006, **4**, 766-69.
12 R. Bakry, R. M. Vallant, M. Najam-ul-Haq, M. Rainer, Z. Szabo, C. W. Huck and G. K. Bonn, *Int. J. Nanomed*., 2007, **2**, 639-49.
13 C. Cha, S. R. Shin, N. Annabi, M. R. Dokemci and A. Khademhosseini, *ACS Nano*, 2013, **7**, 2891-97.
14 M. L. Chen, Y. J. He, X. W. Chen and J. H. Wang, *Bioconjugate Chem.*, 2013, **24**, 387-97.
15 H. Shen, L. Zhang, M. Liu and Z. Zhang, *Theranostics*, 2012, **2**, 283-94.
16 J. H. Liu, L. Cao, P. G. Luo, S. T. Yang, F. Lu, H. Wang, M. J. Meziani, S. A. Haque, Y. Liu, S. Lacher and Y. P. Sun, *ACS Appl. Mater. Interfaces* 2010, **5**, 1384-89.
17 R. Mamiya, E. Noiri, H. Isobe, W. Nakanishi, K. Okamoto, K. Doi, T. Sugaya, T. Izumi, T. Homma and E. Nakamura, *PNAS* 2010, **107**, 5339-44.
18 H. Isobe, W. Nakanishi, N. Tomita, S. Jinno, H. Okayama and E. Nakamura, *Chem.-Asian J.*, 2006, **1**, 167-75.
19 H. Isobe, S. Sugiyama, K. Fukui, Y, Iwasawa and E. Nakamura, *Angew. Chem. Int. Ed.*, 2001, **40**, 3364-67.
20 H. Isobe, W. Nakanishi, N. Tomita, S. Jinno, H. Okayama and E. Nakamura, *Mol. Pharm.*, 2005, **3**, 124-34.
21 M. Brettreich, S. Burghardt, C. Böttcher, T. Bayerl, S. Bayerl and A. Hirsch, *Angew. Chem. Int. Ed*., 2000, **39**, 1845-48.
22 S. Zhou, C. Burger, B. Chu, M. Sawamura, N. Nagahama, M. Toganoh, U. E. Hackler, H. Isobe and E. Nakamura, *Science*, 2001, **291**, 1944-47.
23 C. Burger, J. Hao, Q. Ying, H. Isobe, M. Sawamura, E. Nakamura and B. Chu, *J. Colloid Interface Sci.*, 2004, **275**, 632-41.
24 D. Joester, M. Losson, R. Pugin, H. Heinzelmann, E. Walter, H. P. Merkle and F. Diederich, *Angew. Chem. Int. Ed*., 2003, **42**, 1486-90.
25 S. P. Jones, N. P. Gabrielson, D. W. Pack and D. K. Smith, *Chem. Commun*., 2008, 4700-02.
26 P. Posocco, S. Pricl, S. Jones, A. Barnard and D. K. Smith, *Chem. Sci*., 2010, **1**, 393-404.
27 S. P. Jones, N. P. Gabrielson, C. H. Wong, H. F. Chow, D. W. Pack, P. Posocco, M. Fermeglia, S. Pricl and D. K. Smith, *Mol. Pharm*., 2011, **8**, 416-29.
28 M. Meldal and C. W. Tornøe, *Chem. Rev.*, 2008, **108**, 2952-3015.
29 S. Srinivasachari, K. M. Fichter and T. M. Reineke, *J. Am. Chem. Soc.*, 2008, **130**, 4618-27.
30 C. C. Chu, Y. J. Tsai, L. C. Hsiao and L. Y. Wang, *Macromolecules*, 2011, **44**, 7056-61.

31 A. M. López, F. Scarel, N. R. Carrero, E. Vázquez, A. Mateo-Alonso, T. D. Ros and M. Prato, *Org. Lett.*, 2012, **14**, 4450-53.

32 A. J. Geall and I. S. Blagbrough, *J. Pharm. Biomed. Anal.*, 2000, **22**, 849-59.

33 A. Barnard, P. Posocco, S. Pricl, M. Calderon, R. Haag, M. E. Hwang, V. W. T. Shum, D. W. Pack and D. K. Smith, *J. Am. Chem. Soc.*, 2011, **133**, 20288-300.

34 B. Becker, J. Clapper and K. R. Harkins, J. A. Olson, *Anal. Biochem.*, 1994, **221**, 78-84.

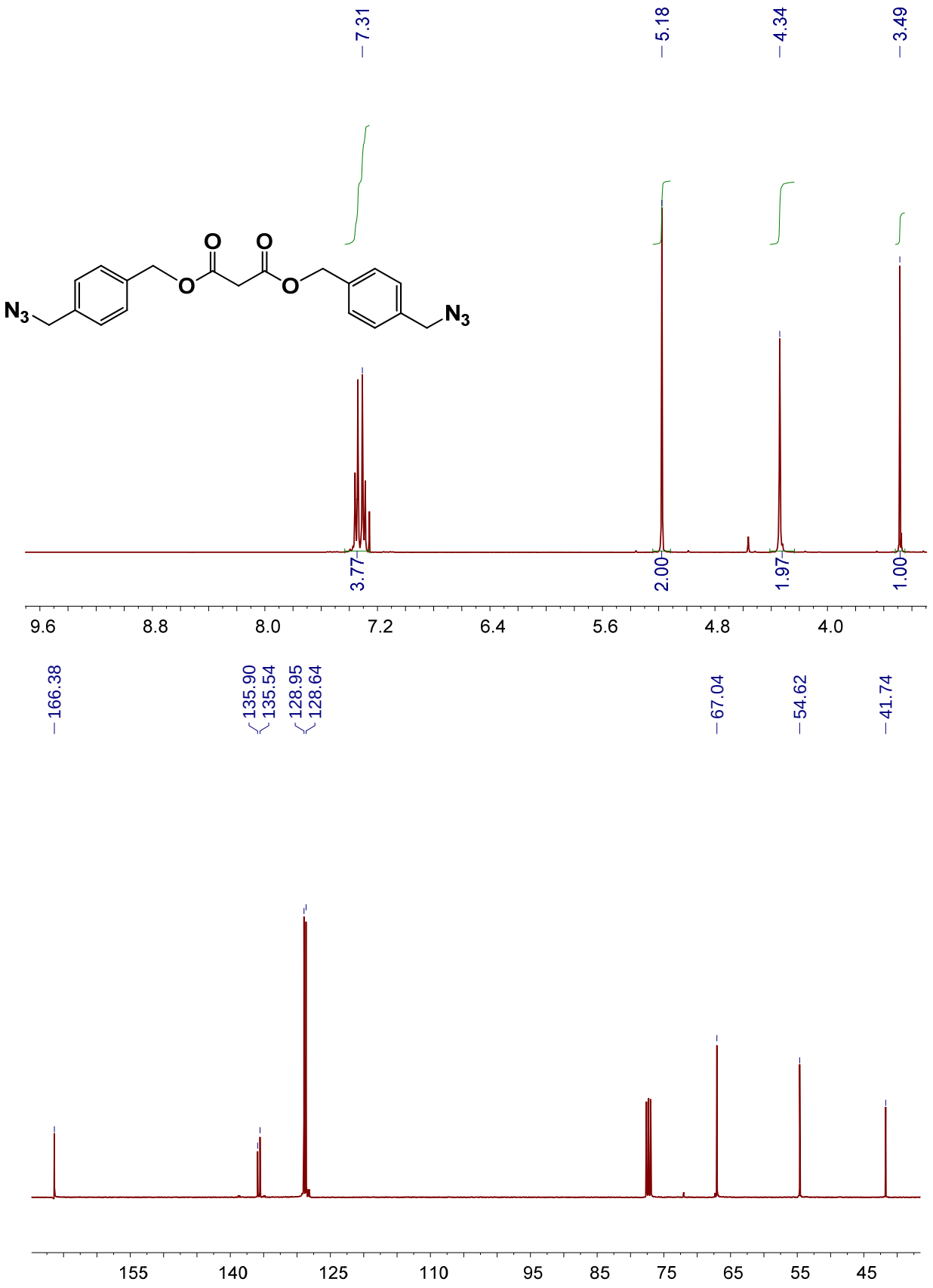

Figure S1. ^{1}H and ^{13}C NMR spectra of compound ***2***.

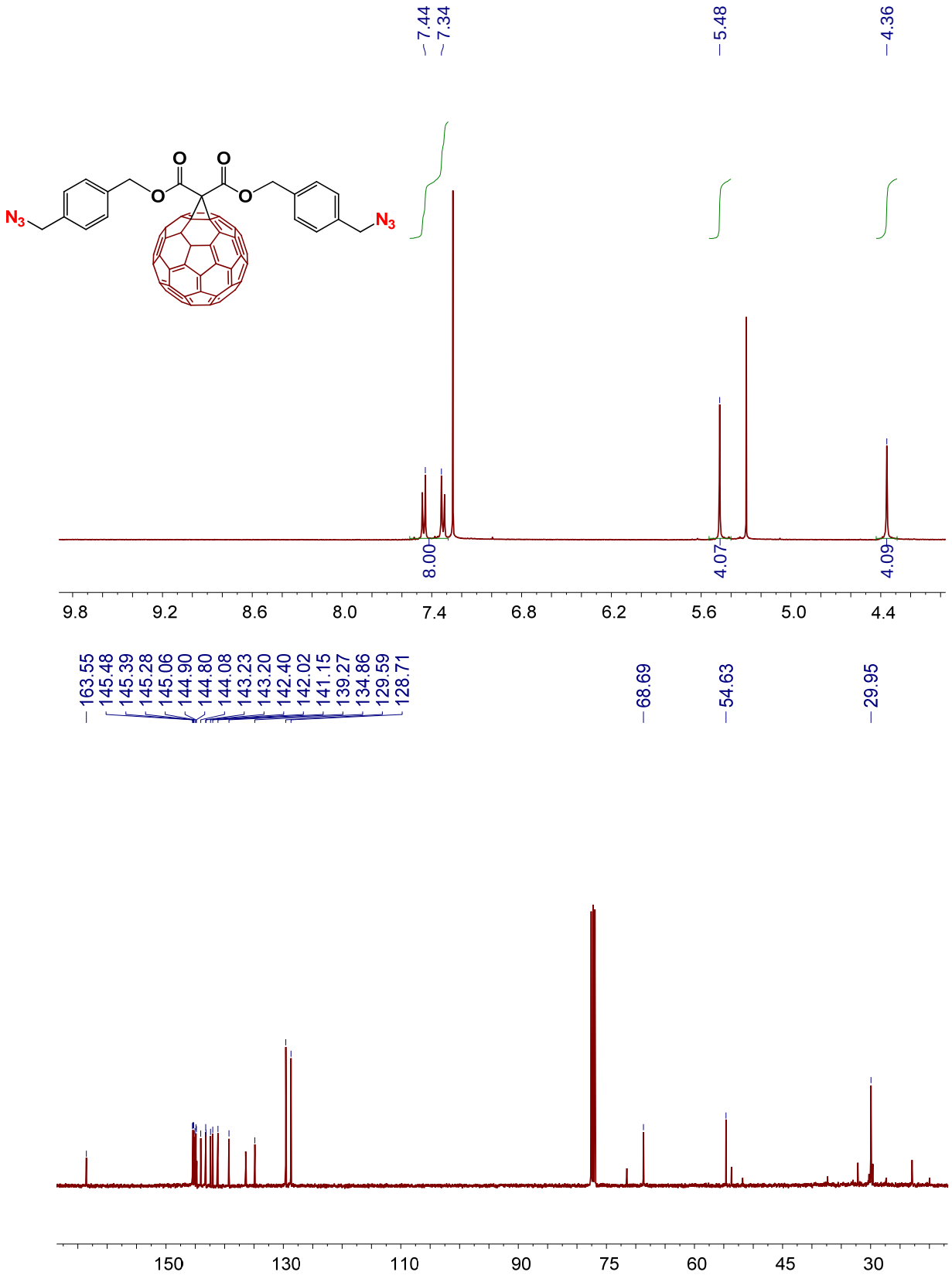

Figure S2. ^{1}H and ^{13}C NMR spectra of compound ***3***.

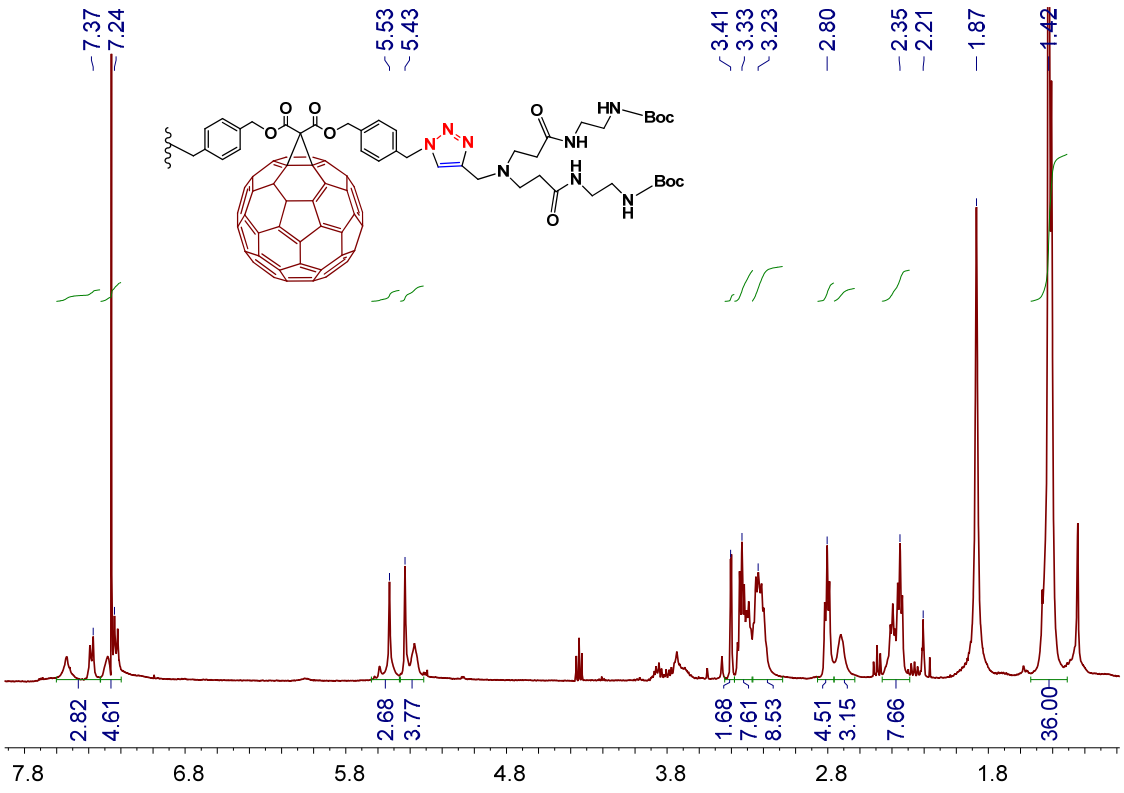

Figure S3. [1]H NMR spectrum of compound Boc-protected ***$C_{60}G_1$***.

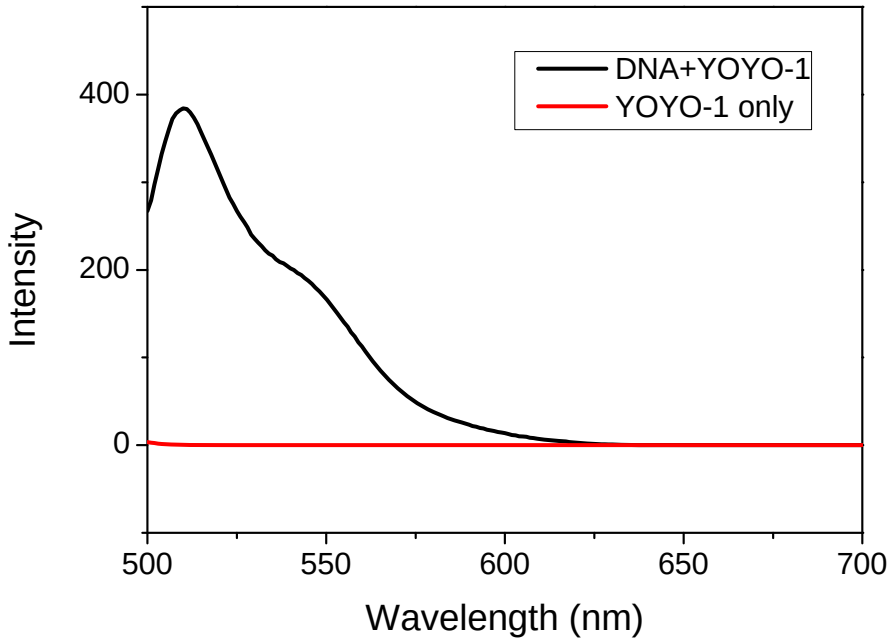

Figure S4. YOYO-1 cyanine-based probe does not emit fluorescence until bound to double-stranded DNA (pEGFP-C1), when the emission intensity for these complexes dramatically increases.

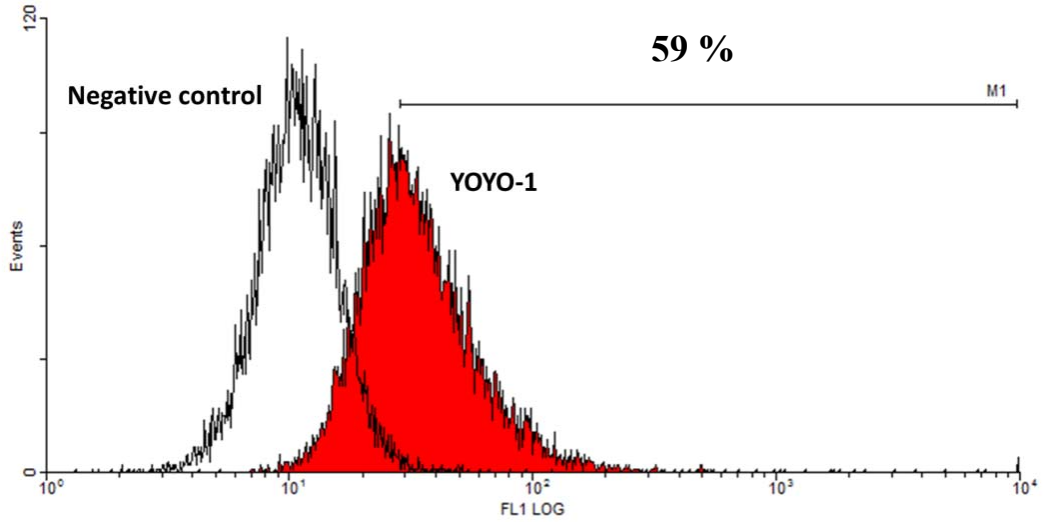

Figure S5. The flow cytometry histogram reveals YOYO-1 self-penetration into the target cell lines without the aid of a vector; and approximately 59% of HeLa cells were YOYO-1 positive, with a mean fluorescence intensity of 48 units.

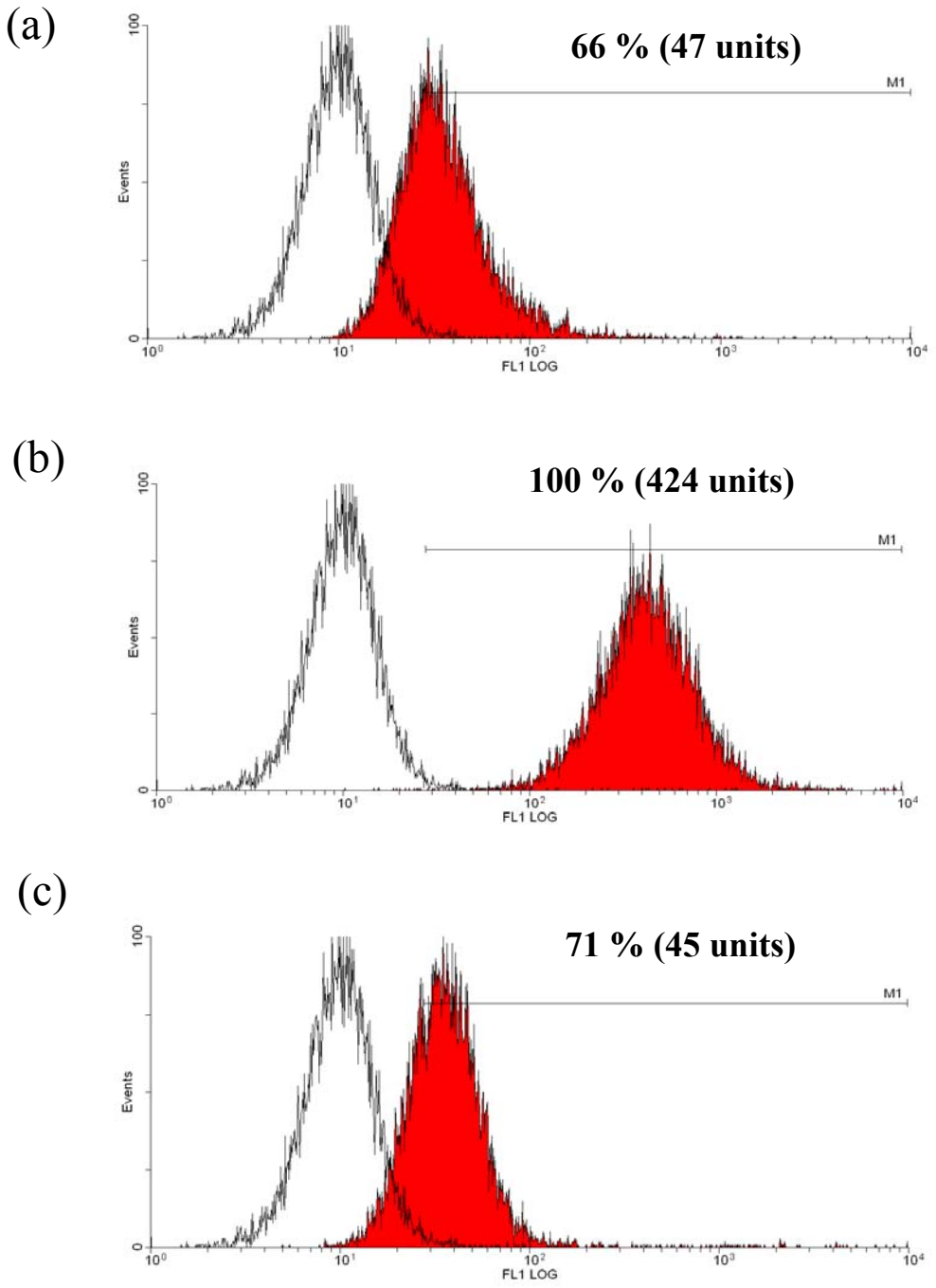

Figure S6. Flow cytometry histograms of HeLa cells internalized by (a) YOYO-1 only, (b) $C_{60}G_1$/ pEGFP-C1/YOYO-1, and (c) G_2/ pEGFP-C1/YOYO-1 at N/P = 2.

國科會補助計畫衍生研發成果推廣資料表

日期:2014/03/20

國科會補助計畫	計畫名稱: 水溶性碳六十衍生物與聚醯胺乙二胺樹枝狀分子在基因轉染上的研究
	計畫主持人: 朱智謙
	計畫編號: 100-2113-M-040-007-MY2　　學門領域: 有機材料

無研發成果推廣資料

100 年度專題研究計畫研究成果彙整表

計畫主持人：朱智謙	計畫編號：100-2113-M-040-007-MY2
計畫名稱：水溶性碳六十衍生物與聚醯胺乙二胺樹枝狀分子在基因轉染上的研究	

成果項目			量化			單位	備註（質化說明：如數個計畫共同成果、成果列為該期刊之封面故事...等）
			實際已達成數（被接受或已發表）	預期總達成數(含實際已達成數)	本計畫實際貢獻百分比		
國內	論文著作	期刊論文	0	0	100%	篇	
		研究報告/技術報告	0	0	100%		
		研討會論文	7	7	100%		
		專書	0	0	100%		
	專利	申請中件數	0	0	100%	件	
		已獲得件數	0	0	100%		
	技術移轉	件數	0	0	100%	件	
		權利金	0	0	100%	千元	
	參與計畫人力（本國籍）	碩士生	0	2	100%	人次	
		博士生	0	0	100%		
		博士後研究員	0	0	100%		
		專任助理	0	1	100%		
國外	論文著作	期刊論文	3	2	100%	篇	
		研究報告/技術報告	0	0	100%		
		研討會論文	2	2	100%		
		專書	0	0	100%	章/本	
	專利	申請中件數	0	0	100%	件	
		已獲得件數	0	0	100%		
	技術移轉	件數	0	0	100%	件	
		權利金	0	0	100%	千元	
	參與計畫人力（外國籍）	碩士生	0	0	100%	人次	
		博士生	0	0	100%		
		博士後研究員	0	0	100%		
		專任助理	0	0	100%		

其他成果 (無法以量化表達之成果如辦理學術活動、獲得獎項、重要國際合作、研究成果國際影響力及其他協助產業技術發展之具體效益事項等，請以文字敘述填列。)	大會邀請演講:第 8 屆國際樹枝狀高分子會議(西班牙馬德里)，發表相關之學術論文。

	成果項目	量化	名稱或內容性質簡述
科教處計畫加填項目	測驗工具(含質性與量性)	0	
	課程/模組	0	
	電腦及網路系統或工具	0	
	教材	0	
	舉辦之活動/競賽	0	
	研討會/工作坊	0	
	電子報、網站	0	
	計畫成果推廣之參與（閱聽）人數	0	

科技部補助專題研究計畫成果報告自評表

請就研究內容與原計畫相符程度、達成預期目標情況、研究成果之學術或應用價值（簡要敘述成果所代表之意義、價值、影響或進一步發展之可能性）、是否適合在學術期刊發表或申請專利、主要發現或其他有關價值等，作一綜合評估。

1. 請就研究內容與原計畫相符程度、達成預期目標情況作一綜合評估

■達成目標

□未達成目標（請說明，以 100 字為限）

□實驗失敗

□因故實驗中斷

□其他原因

說明：

2. 研究成果在學術期刊發表或申請專利等情形：

論文：□已發表 □未發表之文稿 ■撰寫中 □無

專利：□已獲得 □申請中 ■無

技轉：□已技轉 □洽談中 ■無

其他：(以 100 字為限)

3. 請依學術成就、技術創新、社會影響等方面，評估研究成果之學術或應用價值（簡要敘述成果所代表之意義、價值、影響或進一步發展之可能性）(以 500 字為限)

本兩年期計劃第二年的計劃目標為兩性樹枝狀分子的合成製備、DNA 複合體的型態分析與物理化學性質分析、以及初步基因轉染效率的探討。自評目前的研究成果符合原先設定之目標。我們利用高效率的合成方法合成出一系列以碳六十為核心的兩性基因載體，經過初步測試後證明此材料具有不錯的 DNA 轉染效率。基於這些發現，除了能夠發表相關的學術論文之外，也可以積極思考申請專利的可能性。